

Metamagnetics for Visible Wavelengths (491 - 754 nm)

Hsiao-Kuan Yuan, Wenshan Cai, Uday K. Chettiar, Vashista de Silva,

Alexander V. Kildishev, Alexandra Boltasseva*, Vladimir P. Drachev, and Vladimir M. Shalaev

School of Electrical and Computer Engineering and Birck Nanotechnology Center, Purdue University, West Lafayette, Indiana 47907

hyuan@purdue.edu, shalaev@purdue.edu

* *DTU, Research Center COM and Nanophotonics, DK-2800 Kgs. Lyngby, Denmark*

Abstract: We designed, fabricated and experimentally validated a representative number of periodic arrays of magnetically resonant silver nanostrips. Our studies confirmed that the coupled-strip design can provide controllable magnetic responses in the entire visible range.

©2007 Optical Society of America

OCIS codes: (230.3990) Microstructure devices; (160.4760) Optical properties; (999.9999) Meta-materials

Theoretical predictions and experiments show that periodic metal-dielectric composites can exhibit strong magnetic responses and therefore represent a new class of optical metamaterials (optical metamagnetics). For example, a diamagnetic response in the coupled pairs of metal nanorods was originally predicted by Podolskiy et. al. [1]. Other studies predicted and demonstrated magnetic responses from different periodic metal-dielectric composites in the terahertz and infrared spectral ranges [2-5]. Optical metamagnetics with controllable effective permeability are of vital importance for negative refraction, subwavelength waveguides, nanoantennas, optical filters, and optical cloaking. Our recent simulations have showed that pairs of thin silver strips separated by a dielectric spacer could offer an easy way of achieving negative magnetism by coupling near-field modes [6, 7].

First, this paper addresses the effect of metal surface roughness on the effective permeability of the fabricated samples [8]. Then, the study is focused on obtaining magnetic responses across the whole visible spectrum by creating a family of paired-strip samples with varying geometries. The dependence of the magnetic resonance wavelength on the geometric parameters is examined both experimentally and theoretically.

Two samples with a periodic array of pairs of silver strips were fabricated (denoted as Sample A and B) using electron beam lithography. First, a periodic array of thin silver strips was defined on a glass substrate initially coated with a 15-nm film of indium-tin-oxide (ITO) using an electron beam writer. Then, electron beam evaporation was applied to produce a stack of lamellar films on the ITO-coated glass: Sample A, 10-nm alumina, 30-nm silver, 40-nm alumina, 30-nm silver, 10-nm alumina; Sample B, 10-nm alumina, 35-nm silver, 40-nm alumina, 35-nm silver, 10-nm alumina. An FE SEM image of the fabricated structure of Sample A is shown in Fig. 1(a), and Sample B is shown in Fig. 2(a). Finally, a lift-off process was performed to obtain the desired silver strips. To measure the transmission and reflection spectra of the samples, an ultra-stable tungsten lamp (B&W TEK BPS100 and a Glan Taylor prism was placed at the output of the broadband lamp to select the light with desired linear polarization. The signal transmitted (or reflected) from the sample was introduced into a spectrograph (Acton SpectraPro 300i) and eventually collected by a liquid nitrogen cooled CCD-array detector. The transmission and reflection spectra were normalized to a bare substrate and a calibrated silver mirror, respectively. In the TE mode the electric field of the incident light was linearly polarized parallel to the length of silver strips, while in TM mode the electric field was rotated 90 degrees relative to TE case. Measurements of the root-mean square (RMS) of surface roughness using an atomic-force microscope (AFM) indicated that Sample B with a slower deposition rate of 0.5 Å/s resulted in better surface roughness (RMS, 1.5 – 2.5 nm) than Sample A with faster deposition rate of ~2Å/s (RMS, 2 – 6 nm).

Commercial finite element software was used for simulations. The optical constants of silver used in the ideal model have been initially taken from the experimental data [9]. For TE polarization shown in Fig. 1(b), the measured and simulated transmission spectra (ideal model) match well over a broad range of wavelengths. The measured spectra of the TE mode indicate a moderate non-resonant wavelength dependence and a low, almost constant, absorption. In contrast to the TE case, where the optical constants of the bulk silver are used to describe the optical behavior of silver strips, the TM polarization reveals substantial discrepancies in the optical properties (specifically, in absorption) in comparison to the data shown for strips in the ideal model with the permittivity of bulk silver in [9]. This enhanced absorption is due to the roughness features and other imperfections in the fabricated structures. We model the contributions from these imperfections through a wavelength-dependent adjustment factor α such that the permittivity of silver is given by $\epsilon = \epsilon' + i\alpha\epsilon''$. The computed results of the transmission and reflection spectra using the adjusted (imaginary part of) permittivity of bulk silver are shown in Figs. 1(c) and 2(c). The employed adjustment factor α is shown in Fig. 2(b). The negative effective permeability was retrieved by using numerical simulations. In Fig. 1(d) and Fig. 2(d), the negative effective permeability of Sample A and Sample B are -1 at 770 nm and -1.7 at 725 nm, respectively. In both samples at the TM polarization, the loss adjustment is significant for the electric resonance and even large

Table 1. Geometric parameters of the magnetic nanostrip of dies on Sample C

Die #	Bottom Width (w_b)	Average Width (w)	Periodicity (p)	Coverage % *
A	95	50	191	0.50
B	118	69	218	0.54
C	127	83	245	0.52
D	143	98	273	0.52
E	164	118	300	0.55
F	173	127	300	0.58

* Cover ratio is calculated by the ratio of bottom width w_b to the periodicity p .

for the magnetic resonance. At the magnetic resonance, the lower surface roughness of the strips in Sample B requires a lower adjustment ($\max(\alpha) \approx 4$) than for Sample A ($\max(\alpha) \approx 6$). These results indicate that by improving the fabrication methods we can to minimize the imperfections causing the increased losses and obtain a much stronger negative magnetic response.

To achieve meta-magnetism in the whole visible range, Sample C with six dies, labeled A through F (Table 1), was fabricated by using slow deposition rate with a range of strip widths from 50 nm (Die A) to 127 nm (Die F). To qualitatively illustrate the resonance properties of the magnetic dies with different strip widths, we took microscopic images of the each die for two orthogonal polarizations, as shown in Fig. 3. For the resonant TM polarization case (Fig. 3a & 3c), we observe distinct colors in different dies both in transmission mode and reflection mode indicating the different resonant frequencies in different dies. For the non-resonant TE polarization, however, the colors are the same for all dies. In this case the samples act as diluted metals with a behavior similar to perfect metals: more reflection and less transmission at longer wavelengths. This is why the non-resonant images appear blue in transmission mode (Fig. 3b) and red in reflection mode (Fig. 3d). Magnetic resonances are observed in the wavelength range between 491 nm and 754 nm, covering the majority of the visible spectrum. The positions of the resonant wavelengths in TM mode move towards the blue when decreasing the width of the strips from Die F to Die A. This verifies the scaling property of the magnetic structure of coupled nanostrips.

For practical designs and applications, it is desirable to have an analytical expression for the relation between the magnetic resonance wavelength λ_m and the geometric parameters: the thickness of silver t , the thickness of alumina spacer d (refractive index n_d) and the average width of trapezoidal-shape strip pair w . Following the cavity model approach discussed in [10, 11], we obtain the approximate solution:

$$\lambda_m = \sqrt{4 + \frac{n_d^2 w}{\pi t} + \frac{2n_d^2 w^2}{\pi^2 t d}} \eta \lambda_p \quad (1)$$

Here $\lambda_p = 134.6$ nm is the plasma wavelength of silver. Due to the trapezoidal shape and the leakage modes at the sidewalls of the paired strips, the actual resonant wavelength is longer so that an adjustment constant $\eta = 1.28$ is used and λ_m is replaced by λ_m/η .

In Fig. 4 we plot the dependence of the magnetic resonance wavelength λ_m on the average width w of the trapezoidal-shape paired strip samples both from experiments and analytical approaches. The experimental data for λ_m and w is taken from collected spectra and FE SEM. From Fig. 4 we can see that the results obtained from the Eq. (1) analytical method match the experimental data remarkably well. Therefore, the equation can be used as a general recipe for producing paired-strip magnetic metamaterials at any desired optical wavelength. Fig. 6 also exhibits negligible saturation due to size-scaling, which indicates that such a structure is capable of producing optical magnetism at even shorter wavelengths.

In summary, we have improved the surface roughness of silver strips and demonstrated optical magnetic responses across the whole visible spectrum. The resonant properties of a family of such structures with varying dimensions were studied both experimentally and numerically. The obtained dependence of the magnetic resonance wavelength on the geometric parameters provides us with a general recipe for designing such magnetic metamaterials at any desired optical frequency. Additionally, it is possible to tune the magnitude of the effective permeability μ' by changing the coverage percentage of the strips. Therefore, the coupled nanostrips structure can serve as a general building block for producing controllable optical magnetism for various practical implementations.

This work was supported in part by ARO grant W911NF-04-1-0350, NSF-PREM grant #DMR-0611430 and by ARO-MURI award 50342-PH-MUR.

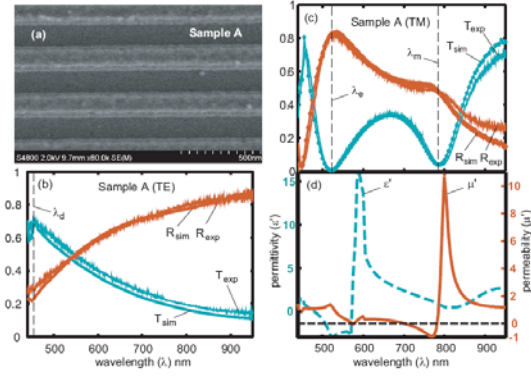


Figure 1: (a) FE SEM of Sample A. (b) Transmission and reflection spectra of Sample A at normal incidence with TE polarization. (c) Transmission and reflection spectra of Sample A at normal incidence with TM polarization compared to spectra obtained from simulations. In this case, ϵ'' of the silver strips was adjusted to match excessive losses. (d) The real part of the effective permeability (μ') and effective permittivity (ϵ').

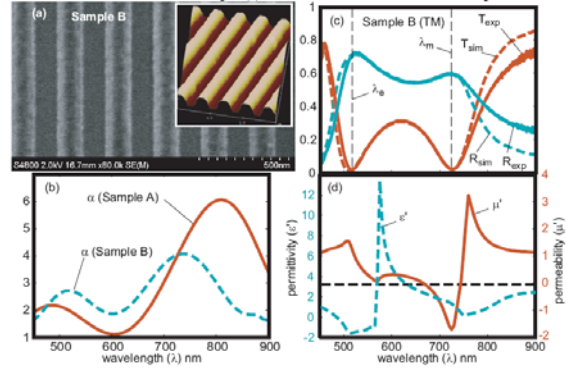


Figure 2: (a) FE SEM/AFM of Sample B. (b) The loss-adjustment factor α for Samples A and B. Sample A demonstrates more loss in comparison to bulk metal [9]. (c) Transmission and reflection spectra of Sample B at normal incidence with TM polarization compared to spectra obtained from simulations. In this case, ϵ'' of the silver strips was adjusted to match excessive losses. (d) The real part of the effective permeability (μ') and effective permittivity (ϵ').

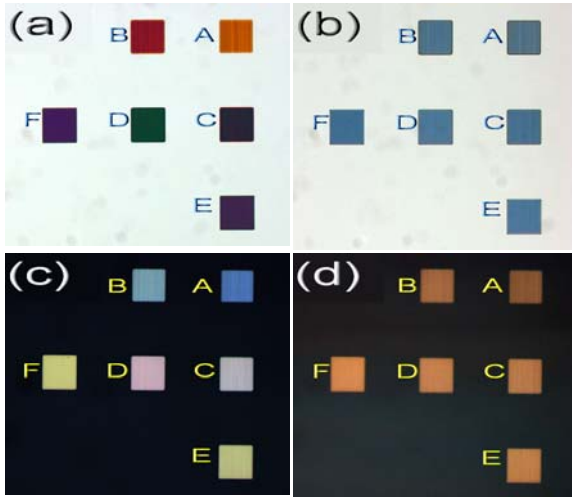


Figure 3: Optical microscopy images of the magnetic samples for two orthogonal polarizations. (a) Transmission mode with TM polarization; (b) Transmission mode with TE polarization; (c) Reflection mode with TM polarization; (d) Reflection mode with TE polarization. Letters A-F correspond to the sample naming in Table 1.

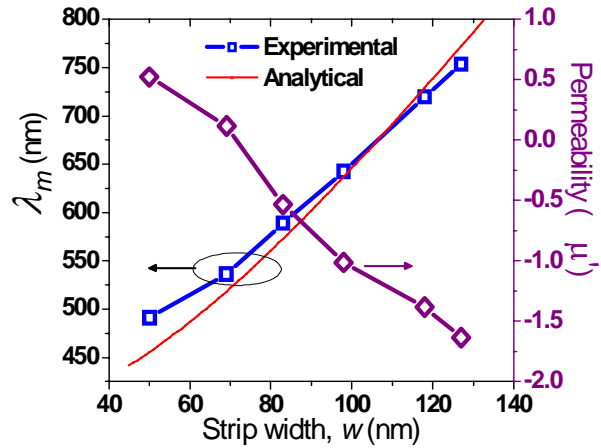


Figure 4: The dependence of the magnetic resonance wavelength λ_m on the average width w of the trapezoidal-shape paired strip samples, and the minimum values of permeability μ' for the six dies around λ_m . Square: experimental data for λ_m as a function of w from Fig. 5 (a,b); Solid line: analytical $\lambda_m(w)$ relationship determined by Eq. (1); Diamond: retrieved minimum effective permeability for each sample.

References

- [1] V.A. Podolskiy, A.K. Sarychev, and V.M. Shalaev, "Plasmon modes in metal nanowires and left-handed materials," *J. Nonlinear Opt. Phys. Materials* **11**, 65-74 (2002).
- [2] J. Zhou, L. Zhang, G. Tuttle, T. Koschny, and C. M. Soukoulis, "Negative index materials using simple short wire pairs," *Phys. Rev. B* **73**, 041101(R) (2006).
- [3] T. J. Yen, W. J. Padilla, N. Fang, D. C. Vier, D. R. Smith, J. B. Pendry, D. N. Basov, and X. Zhang, "Terahertz magnetic response from artificial materials," *Science* **303**, 1494-1496 (2004).
- [4] S. Linden, C. Enkrich, M. Wegener, J. Zhou, T. Koschny, and C. M. Soukoulis, "Magnetic response of metamaterials at 100 Terahertz," *Science* **306**, 1351-1353 (2004).
- [5] C. Enkrich, M. Wegener, S. Linden, S. Burger, L. Zschiedrich, F. Schmidt, J. F. Zhou, Th. Koschny, and C. M. Soukoulis, "Magnetic metamaterials at telecommunication and Visible frequencies," *Phys. Rev. Lett.* **95**, 203901 (2005).
- [6] U. K. Chettiar, A. V. Kildishev, T. A. Klar, and V. M. Shalaev, "Negative index metamaterial combining magnetic resonators with metal films," *Opt. Express* **14**, 7872-7877 (2006).
- [7] G. Shvets and Y. A. Urzhumov, "Negative index meta-materials based on two-dimensional metallic structures," *J. Opt. A* **8**, S122 (2006).
- [8] H. K. Yuan, U. K. Chettiar, W. Cai, A. V. Kildishev, A. Boltasseva, V. P. Drachev, V. M. Shalaev, "A Negative Permeability Material at the Red Light," *Opt. Express* **15**, 1706-1083 (2007).
- [9] P. B. Johnson and R. W. Christy, "Optical constants of the noble metals," *Phys. Rev. B* **6**, 4370-4379 (1972).
- [10] Bahl, I. J. & Bhartia, P. *Microstrip Antennas* (Artech House, Boston, 1980).
- [11] Lomakin, V., Fainman, Y., Urzhumov, Y. & Shvets, G. Doubly negative metamaterials in the near infrared and visible regimes based on thin film nanocomposites. *Opt. Express* **14**, 11164-11177 (2006).